



Synthesizing higher-capacity hard-carbons from cellulose for Na- and K-ion batteries

Journal:	<i>Journal of Materials Chemistry A</i>
Manuscript ID	TA-COM-06-2018-005203.R1
Article Type:	Communication
Date Submitted by the Author:	06-Jul-2018
Complete List of Authors:	Yamamoto, Hijiri; Tokyo University of Science, Department of Applied Chemistry Muratsubaki, Shotaro; Tokyo University of Science, Department of Applied Chemistry Kubota, Kei; Tokyo University of Science, Department of Applied Chemistry Fukunishi, Mika; Tokyo University of Science, Department of Applied Chemistry Watanabe, Hiromu; Mitsubishi Chemical Corporation Kim, Jungmin; Mitsubishi Chemical Corporation Komaba, Shinichi; Tokyo University of Science, Department of Applied Chemistry



Journal Name

COMMUNICATION

Synthesizing higher-capacity hard-carbons from cellulose for Na- and K-ion batteries

Received 00th January 20xx,
Accepted 00th January 20xx

Hijiri Yamamoto,^a Shotaro Muratsubaki,^a Kei Kubota,^a Mika Fukunishi,^a Hiromu Watanabe,^b
Jungmin Kim,^b and Shinichi Komaba^{a*}

DOI: 10.1039/x0xx00000x

www.rsc.org/

Non-graphitizable hard carbons are synthesized through carbonization of glucose, sucrose, maltose, cellulose, glycogen, and amylopectin. Cellulose-derived carbon delivers superior reversible sodiation capacity, and optimal carbonization for higher capacity Na-ion battery is found to be two-step heating of cellulose at 275 °C and 1300–1500 °C in air and argon, respectively. The hard carbon delivers the higher reversible capacity of 353 mAh g⁻¹ in Na cell. The 275 °C heating is important to regulate dehydration and cross-linkage degrees of cellulose, which affect nano-scale structure of hard carbons. The cellulose-derived carbons deliver 523 and 290 mAh g⁻¹ in Li and K cells, respectively.

Based on earlier challenges of reversible electrochemical insertion of sodium into disordered-carbon,^{1, 2} we demonstrated the long-life and high-capacity hard carbon (non-graphitizable carbon) electrode for Na-ion battery application.^{3, 4} Among sodium insertion materials reported so far, hard carbon emerges as one of the most promising materials for the negative electrode because of totally-balanced performances in terms of reversible capacity, electronic conductivity, working potential, cycle life, and abundant resource.^{5, 6} Reversible sodiation capacity of hard carbons typically ranges from 200 to 330 mAh g⁻¹ below 1.5 V vs. Na⁺/Na, and sodium insertion mechanisms into hard carbon have been studied while atomic-scale structure of hard carbon is still a debatable subject.^{3, 4, 7-9} The structure of hard carbon depends on synthesis conditions such as carbon sources and carbonization temperatures,¹⁰ resulting in the difficulty to construct a universal structural model of hard carbon. In general, hard carbon is composed of two characteristic domains; stacked hexagonally-bounded carbon sheets and micropores (nano-sized pores), i.e. interstitial spaces of the stacked carbons.

Recently, some of biowastes have been used as starting materials for one-step pyrolysis at 700 - 1500 °C to synthesize higher-capacity hard carbons, which deliver 300 mAh g⁻¹ or higher capacity.^{9, 10} As we reported,^{10, 11} sucrose, cellulose, lignin, bio-wastes containing cellulose and lignin, and their chemically modified precursors are pyrolyzed to tailor high-energy hard carbons, demonstrating 250–330 mAh g⁻¹ of reversible capacity. In this study, we investigate dependence of sodium battery performance of saccharide- and cellulose-derived hard carbons on two-step carbonization of cellulose and correlate their electrochemical performance with nanostructure relating to dewatering and cross-linkage of cellulose.¹² The optimal hard carbons are demonstrated for higher energy Na- and K-ion batteries.

Hard carbon was synthesized via two-step heat-treatment; pre-heating and carbonization steps. Precursors were prepared by pre-heating reagent-grade saccharide powders at 180, 275, 300, and 350 °C for 12 h in the furnace. The precursors were further carbonized at 1300 °C for 1 h in Ar. For electrochemical test, hard carbon powder was mixed with sodium polyacrylate (PANa, Kishida Chemical) binder at a weight ratio of 95:5 with deionized water. The resulting slurry was pasted onto Al foils (Cu foils for Li cell) and dried carefully. R2032-type Li, Na, and K cells were assembled in an Ar-filled glove box. Electrolyte solutions used were 1.0 mol dm⁻³ NaPF₆ propylene carbonate (PC) and 1.0 mol dm⁻³ KN(SO₂F)₂ (KFSA) EC:diethyl carbonate (DEC) (1:1 v/v). Galvanostatic tests of the Li/Na/K cells at 25 mA g⁻¹ were performed at approximately 25 °C. Constant voltage at 0.002 V was applied for 8 h after the galvanostatic reduction to minimize influence of polarization of the cells. More detailed conditions are shown in **Supporting Information**.

We first synthesized and compared six hard-carbons derived from saccharides. We selected a series of saccharides consisting of glucose monomer unit(s); glucose, sucrose, maltose, cellulose, glycogen and amylopectin. Molecular structure and weight of the saccharides used are shown in **Supporting Information, Figures S1 and S2**. The selected polysaccharides, cellulose, glycogen and amylopectin, possess

^a Department of Applied Chemistry, Tokyo University of Science, Shinjuku, Tokyo 162-8601, Japan. *E-mail: komaba@rs.kagu.tus.ac.jp

^b Mitsubishi Chemical Corporation, Yokohama, Kanagawa 227-8502, Japan.

†Electronic Supplementary Information (ESI) available: experimental details, detailed synthesis observation and characterizations, and electrochemical data. See DOI: 10.1039/x0xx00000x

different monomer-monomer linkage bonds with different branch structures of polymer chain. White powders of these saccharides were treated under the same carbonization conditions, i.e. pre-treatment at 180 °C in air and following carbonization at 1300 °C in Ar. Although differently colored precursors are obtained by the pre-treatment, carbon powders having similar particle sizes of several micrometers are prepared by the carbonization as seen in **Figure S2**, evidencing that they are non-graphitizable carbons (see **Figures S3**).

Figure 1a compares the initial charge-discharge curves (corresponding to sodium insertion-extraction into/from hard carbons in a Na-ion cell). All of the hard carbons show similar voltage curves at the first cycle as observed for hard carbons.^{9, 10} Glucose-, sucrose-,¹¹ maltose-, cellulose-, glycogen-, and amylopectin-derived hard carbon delivers high reversible capacities of 296, 303, 310, 317, 305, and 298 mAh g⁻¹, respectively, with high coulombic efficiency of ca. 87 – 94 %. The greater capacity and efficiency are achieved for the cellulose case. The broad diffraction in XRD and calculated *d* spacing ranging between 3.75 and 3.86 Å in **Figures S3** prove that cellulose-derived carbon shows the largest *d* value, which is likely caused by the different polymerization and branch degrees. The capacity below 0.15 V corresponding to sodium clustering in the micropore^{8, 10, 13} is brought out by using cellulose (see **Figure S4**).

The influence of preheating prior to carbonization was investigated for cellulose case. XRD result of **Figure 1b** reveals

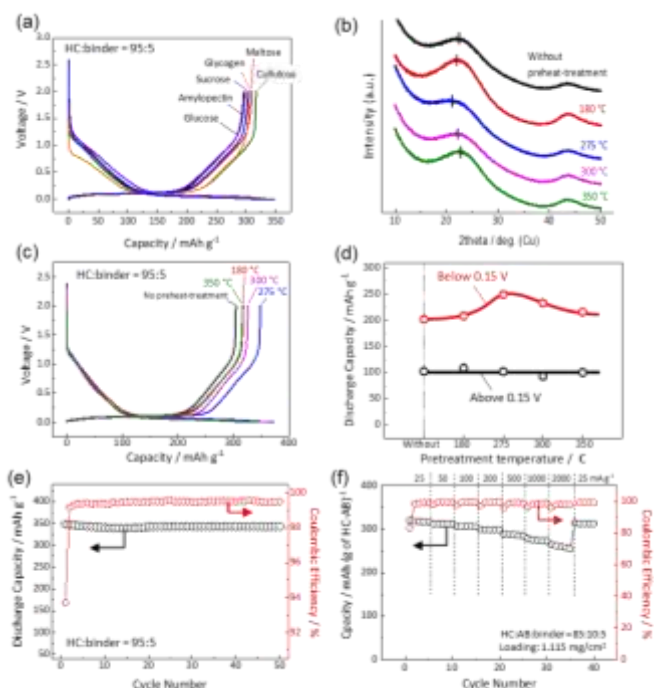


Figure 1 (a) Initial sodiation and desodiation curves of hard carbons prepared by heating saccharides at 180 and 1300 °C of pre-treatment and post-carbonization, respectively. (b) XRD patterns, (c) first sodiation and desodiation curves, (d) divided reversible capacities above and below 0.15 V of cellulose-derived hard carbons prepared at different preheating temperatures which are inserted in the figure followed by post-carbonization at 1300 °C. (e) Cycleability and (f) rate capability of the hard carbon prepared by heating cellulose at 275 and 1300 °C as pre- and post-treatment, respectively.

the formation of hard carbons despite preheating temperatures of 180 – 350 °C which are selected from thermogravimetry data of cellulose pyrolysis in air as shown in **Figures S5 and S6**. According to previous literatures,^{12, 14, 15} thermal dewatering and formation of covalent cross-linkage of cellulose molecules proceeds at about 300 °C, and then the highly cross-linked product is formed at 350 °C; additionally the cross-linkage structure is developed when raising temperature slowly. In **Table 1** and **Figure S7**, elemental analysis proves decrease in hydrogen and oxygen contents which agrees with the literature, and high specific surface area is found by preheat-treatment at 275 and 300 °C. In spite of the higher surface area of > 500 m² g⁻¹, the high efficiency of ~ 90 % at first cycle was attained which would be due to the pre-formed SEI effect with PANa binders.^{10, 16} While color of the precursors at 180 and 275 °C appears to be yellow and black (**Figure S8**), insignificant difference in particle size of the carbons was noted in **Figures S9 and S10**. However, **Figure 1c** reveals the remarkable impact of preheat temperatures on the reversible capacity. The preheating at 275 °C demonstrates the highest capacity of 350 mAh g⁻¹. From **Table 1**, the highest-capacity carbon has larger surface area, wider interlayer distance, and relatively large nano-sized pores of ca. 1.2 nm (see also **Figures S11 and S12**). **Figure 1d** shows the increase of the low-potential capacity below 0.15 V for the 275 °C sample, which is consistent with the larger size of micropore estimated from SAXS results similar to other hard carbons.^{9, 10} As described above, the precursor obtained at 275 °C has greatly cross-linked structure, which is proved by the definite appearance of aromatic carbons and disappearance of pristine cellulose in the precursor evidenced with solid-state ¹³C nuclear magnetic resonance measurement (see **Figure S13**). The cross-linkage, which interrupts graphitization during carbonization,¹² induces the successful micropore formation contributing to the capacity increase as described below. No capacity decay over fifty cycles at least and excellent rate-capability at 2000 mA g⁻¹ are demonstrated in **Figures 1e and 1f**. Consequently, the performance is satisfactory for practical battery application.

Influence of carbonization temperature for the 275 °C precursor is investigated and the hard carbons are

Table 1. Comparison of elemental analysis, N₂ adsorption, XRD, and SAXS results of precursors and hard carbons obtained at different temperatures.

Preheat-treatment temperature / °C	Carbonization temperature / °C	H/C	O/C	BET surface area / m ² g ⁻¹	Average interlayer distance / Å	Radius of micropore / Å
Without	-	0.154	1.100	1.03	-	-
180	-	0.150	1.079	0.84	-	-
275	-	0.046	0.540	217	-	-
300	-	0.036	0.493	109	-	-
350	-	0.030	0.513	1.80	-	-
Without	1300	-	-	78	3.83	7.5
180	1300	-	-	150	3.84	7.5
275	1300	-	-	506	3.91	12.4
300	1300	-	-	476	3.83	14.3
350	1300	-	-	14	3.76	11.8

Table 2 Comparison of elemental analysis, N₂ adsorption, XRD, and SAXS results of hard carbons obtained at different temperatures of carbonization after pretreatment at 275 °C.

Carbonization temperature / °C	BET surface area / m ² g ⁻¹	Average interlayer distance / Å	Radius of micropore/Å
700	693	4.31	4.4
900	677	4.17	8.1
1100	577	3.81	11.1
1300	506	3.89	12.4
1500	77	3.82	12.5

characterized as presented in Table 2. The results exhibit that carbonization at higher temperature leads to decrease in surface area, shrinkage in interlayer space, and increase in micropore radii (see also Figure S14). This trend is coincident with previous results of the argan-derived carbons.¹⁰ Figure 2a shows the first sodiation-desodiation curves, indicating that lower carbonization temperature than 1100 °C results in lower capacity of < 260 mAh g⁻¹ and lower coulombic efficiency due to the large specific area and potential hysteresis like lithium case.¹⁷ Hard carbons obtained at 1300 and 1500 °C deliver 351 and 353 mAh g⁻¹ of reversible capacity with negligible potential hysteresis.

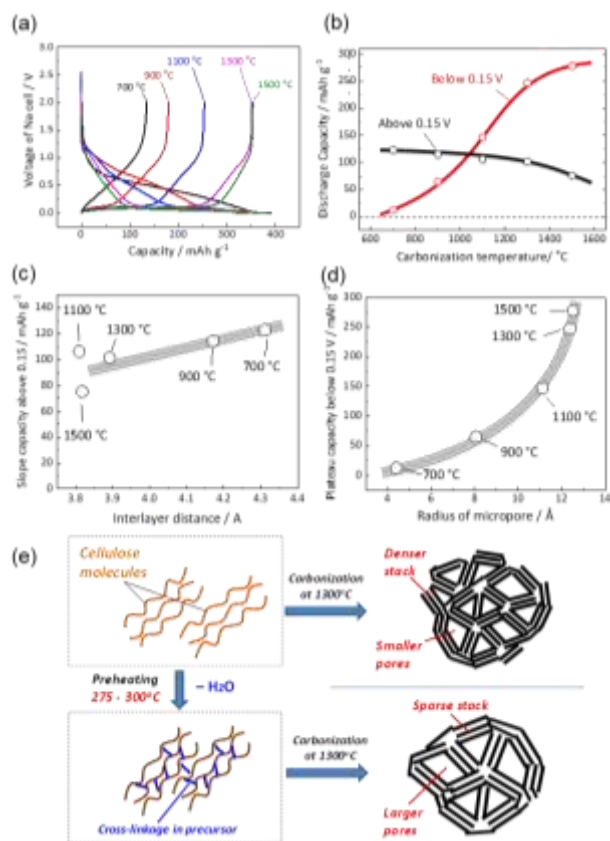


Figure 2 Dependence of reversible capacity of hard carbons on carbonization temperatures of the 275 °C precursors; (a) first sodiation and desodiation curves in the CC-CV mode, (b) reversible capacities divided the potential regions below and above 0.15 V, relation (c) between slope capacity (2.0 – 0.15 V) and interlayer distance and (d) between plateau capacity (0.002 – 0.15 V) and radius of micropore, and (e) schematic draw of molecular structure change during hard-carbon preparation from cellulose depending on preheat treatment.

Figure 2b shows the relation between the carbonization temperature and divided capacities at 0.15 V.¹⁰ The capacity above and below 0.15 V decreases and increases as a function of temperature. As seen in Figures 2c and 2d, the former and latter capacities correlate with the interlayer distance and micropore size estimated from XRD and SAXS, respectively. The plateau capacity predominantly increases up to 270 mAh g⁻¹ with the increase of micropore size whereas the slope capacity slightly varies between 70 – 130 mAh g⁻¹ in Figures 2b – 2d. This temperature trend is schematically summarized in Figure S15. Although the similar tendency was reported previously,^{2, 10} we achieved the highest capacity of 353 mAh g⁻¹ by utilizing the strategic crosslinked precursor.

Figure 2e shows the schematic illustration presenting the impact of the cross-linkage on hard-carbon structure. Preheating at 275 – 300 °C in air causes the dehydration and crosslink between the polymer chains. We believed that the covalent linkage promotes pillar effect resulting in the larger

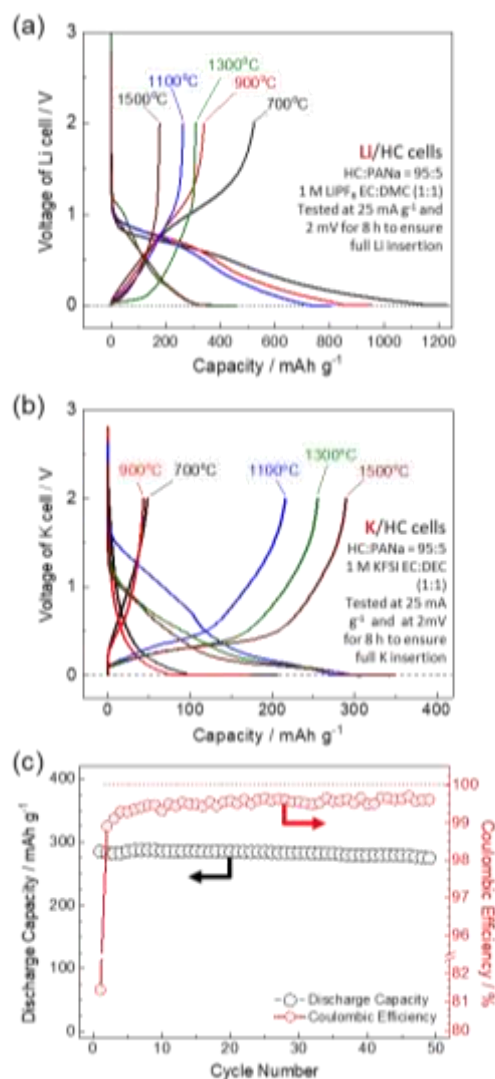


Figure 3 Charge and discharge curves of cellulose-derived hard carbons (pretreatment at 275 °C and post-treatment at 700 – 1500 °C) with 5 wt% PANA binder in (a) Li and (b) K cells tested at a current rate of 25 mA g⁻¹ under CC-CV lithiation and potassiation, respectively, and (c) capacity retention of the hard carbon prepared at 275 °C and 1300 °C K cell.

pores and wider interspace between the stacked carbon sheets, which leads to the higher capacity.⁹ When pristine cellulose is directly carbonized without preheating, the dense stack and smaller pores are formed in hard carbons showing the lower redox activity.

The hard carbons are further examined in Li and K cells in **Figure 3**. High capacity lithium insertion of ca. 500 mAh g⁻¹ is confirmed for the 700 °C samples, and the capacity decreases with raising the carbonization temperature consistent with previous study.¹⁷ Reversible potassium insertion capacity increased from 50 to 290 mAh g⁻¹ with raising carbonization temperature. The optimal carbon synthesized by carbonizing the 270 °C-precursor at 1500 °C demonstrated higher capacity compared to the previous report¹⁸ with good retention and higher coulombic efficiency than 99.5 % over 50 cycles. The cellulose-derived carbons deliver higher capacity compared to sucrose-derived carbons in K cells and the pretreatment at 275 °C is efficient to increase potassiation capacity as proved by **Figure S16**. By comparing the initial Coulombic efficiencies of hard carbons in Li, Na, and K cells, the much lower efficiency is observed in Li cells especially for hard carbons formed at 700, 900, and 1100 °C. Because Li⁺ ion is stronger Lewis acid than Na⁺ and K⁺ ions, the irreversibility should be due to entrapment of the Li⁺ ions at the functional groups in hard carbons.¹⁹ Self-discharge test of the fully potassiated electrode verified that the capacity of > 90% is retained after one-month storage comparable to Li and Na cases (see **Figure S17**) evidencing good passivation. The potassium storage mechanism and surface passivation are under investigation.

Conclusions

Saccharide-derived hard-carbons are comparatively studied for the battery application. Cellulose-derived hard carbons show higher capacity, and one of important factors is found to be pre-treatment of cellulose to introduce cross-linkage. The optimization facilitates the higher reversible capacity of 353 and 290 mAh g⁻¹ in Na and K cells, respectively. Further study on the relation between structure and redox mechanism is in progress to realize higher energy sodium- and potassium-ion energy storage.

Acknowledgements

The authors are grateful to Dr. Saiko Arai, Mitsubishi Chemical Corporation, for the ¹³C NMR measurement. S. K. thanks Ms. Azusa Kamiyama for her assistance in manuscript preparation. This study is partly granted by JST A-STEP, JSPS KAKENHI (JP16K14103 and JP16K18242), and MEXT program "Elements Strategy Initiative to Form Core Research Center" (since 2012).

Conflicts of interest

There are no conflicts to declare.

References

1. M. M. Doeff, Y. Ma, S. J. Visco and L. C. De Jonghe, *Journal of the Electrochemical Society*, 1993, **140**, L169-L170.
2. K. Kubota, M. Dahbi, T. Hosaka, S. Kumakura and S. Komaba, *The Chemical Record*, 2018, **18**, 459-479.
3. N. Yabuuchi, K. Kubota, M. Dahbi and S. Komaba, *Chemical Reviews*, 2014, **114**, 11636-11682.
4. S. Komaba, W. Murata, T. Ishikawa, N. Yabuuchi, T. Ozeki, T. Nakayama, A. Ogata, K. Gotoh and K. Fujiwara, *Advanced Functional Materials*, 2011, **21**, 3859-3867.
5. K. Kubota and S. Komaba, *Journal of the Electrochemical Society*, 2015, **162**, A2538-A2550.
6. C. Vaalma, D. Buchholz, M. Weil and S. Passerini, *Nature Reviews Materials*, 2018, **3**, 18013.
7. D. Stevens and J. Dahn, *Journal of the Electrochemical Society*, 2001, **148**, A803-A811.
8. R. Morita, K. Gotoh, M. Fukunishi, K. Kubota, S. Komaba, N. Nishimura, T. Yumura, K. Deguchi, S. Ohki and T. Shimizu, *Journal of Materials Chemistry A*, 2016, **4**, 13183-13193.
9. D. Saurel, B. Orayech, B. Xiao, D. Carriazo, X. Li and T. Rojo, *Advanced Energy Materials*, 2018, **2018**, in-press.
10. M. Dahbi, M. Kiso, K. Kubota, T. Horiba, T. Chafik, K. Hida, T. Matsuyama and S. Komaba, *Journal of Materials Chemistry A*, 2017, **5**, 9917-9928.
11. M. Dahbi, N. Yabuuchi, K. Kubota, K. Tokiwa and S. Komaba, *Physical Chemistry Chemical Physics*, 2014, **16**, 15007-15028.
12. K. Kobayashi, *Tanso*, 1970, **1970**, 21-30.
13. J. M. Stratford, P. K. Allan, O. Pecher, P. A. Chater and C. P. Grey, *Chemical Communications*, 2016, **52**, 12430-12433.
14. W. Chaiwat, *Doctoral thesis, Kyoto University*, 2010.
15. F. J. Norton, G. D. Love, A. J. Mackinnon and P. J. Hall, *Journal of Materials Science*, 1995, **30**, 596-600.
16. W. Zhang, M. Dahbi and S. Komaba, *Current Opinion in Chemical Engineering*, 2016, **13**, 36-44.
17. J. R. Dahn, T. Zheng, Y. Liu and J. S. Xue, *Science*, 1995, **270**, 590-593.
18. Z. Jian, Z. Xing, C. Bommier, Z. Li and X. Ji, *Advanced Energy Materials*, 2016, **6**, 1501874.
19. E. Buiel and J. R. Dahn, *Electrochimica Acta*, 1999, **45**, 121-130.

TOC graphics

